CONSERVAR PATRIMÓNIO

ENCoRE 4th Ulrich Schiessl PhD Colloquium
4º Colóquio de Doutorandos Ulrich Schiessl da ENCoRE
in Press **ARTICLE / ARTIGO**

Applicability of X-ray imaging to monitor the internal condition of waterlogged archaeological wood – pre-, intra-, and post-conservation

Uso da imagem de raios X para monitorizar a condição interna de madeira arqueológica encharcada – pré-, intra- e pós-conservação

JAMES HARVIE [1*]
JENS GREGERS AAGAARD [1]
JÖRG STELZNER [2]
SUSAN BRAOVAC [3]
INGRID STELZNER [4]
NANNA BJERREGAARD PEDERSEN [1]

1. Royal Danish Academy, Institute of Conservation, Esplanaden 34, 1263, Copenhagen K, Denmark
2. IMPALA (Imaging Platform at LEIZA), Ludwig-Lindenschmit-Forum 1, 55116 Mainz, Germany
3. Museum of Cultural History, University of Oslo, Kabelgata 34, 0580, Oslo, Norway
4. Leibniz-Zentrum für Archäologie, Mainz, Germany

**jaha@kglakademi.dk*

Abstract

During conservation treatment, the greatest threat to waterlogged archaeological wooden (WAW) objects is collapse and/or shrinkage, which can occur during the drying process. Recent work undertaken by the CuTAWAY project revealed, using Micro-computed tomography (micro-CT), that the extent of adverse structural changes found internally in conserved WAW was far greater than generally anticipated. Suggesting a need for conservators to be able to monitor and assess the internal condition of WAW, prior to, during and after treatment. In this study, it was found that X-ray imaging offers a faster and more widely available alternative to micro-CT scanning. While the images are lower resolution than their micro-CT counterparts, they were able to make out the vast majority of internal damages present in a range of samples during various stages of treatment. However, the correct interpretation of internal damage in the X-ray images requires an underlying knowledge of the wood material.

KEYWORDS
Waterlogged archaeological wood
Conservation
Condition
X-ray

Resumo

Durante o tratamento de conservação, a maior ameaça aos objetos arqueológicos de madeira saturada de água (WAW) é o colapso e/ou contração, que podem ocorrer durante o processo de secagem. Trabalhos recentes realizados pelo projeto CuTAWAY revelaram, utilizando micro-tomografia computadorizada (micro-CT), que a extensão das alterações estruturais adversas encontradas internamente nos WAW conservados era muito maior do que o geralmente previsto. Sugerindo a necessidade de os conservadores monitorizarem e avaliarem a condição interna dos WAW antes, durante e após o tratamento. Neste estudo, verificou-se que a imagem por raios X oferece uma alternativa mais rápida e amplamente disponível à micro-CT. Embora as imagens tenham uma resolução inferior às obtidas por micro-CT, permitiram identificar a grande maioria dos danos internos presentes numa série de amostras durante várias etapas do tratamento. No entanto, a interpretação correta dos danos internos nas imagens de raios X requer um conhecimento prévio do material lenhoso.

PALAVRAS-CHAVE
Madeira arqueológica saturada de água
Conservação
Condição
Raios X

Introduction

Wood heritage objects provide an invaluable insight into the evolutionary history of homo sapiens and past cultures. Wood objects used "from cradle to coffin" throughout history offer a rich and varied contribution to the archaeological record [1]. Both the material analysis of the worked wood surface and analysis of the internal structure of wood, as takes place in the field of dendrochronology to date and to create climate models, can provide a great deal of information about our past [2].

Wood survives in the archaeological record only in extreme climate conditions, where the common fast-acting wood degraders cannot operate or are severely inhibited [3]. In temperate regions, waterlogged anaerobic environments are the most common of these extreme conditions. Here, wood is primarily degraded by a slow-acting form of bacteria. Known as erosion bacteria, these bacteria degrade the cellulose and hemicellulose-rich secondary wall of the wood cell wall, leaving the compound middle lamella intact [3-4]. This results in waterlogged archaeological wood (WAW) appearing in good condition when first excavated. However, upon uncontrolled drying, internal stresses can develop in wood. These are primarily the result of the collapse of wood cells during drying above the fibre saturation point and/or the uneven dimensional change of the wood cells below the fibre saturation point, as the wood cell walls shrink at different rates and times due to uneven drying fronts and the anisotropic nature of wood [5-6]. When these drying stresses exceed the weakened material strength of the degraded wood, adverse structural changes will occur.

The primary aim of conserving WAW is to prevent these adverse structural changes during the drying process. This is typically achieved using a conservation agent, commonly polyethylene glycol (PEG), which impregnates the wood cell lumen and fills the wood cell wall, strengthening the degraded wood material and preventing significant shrinkage [7-9]. This is most often followed by a controlled drying method, such as freeze-drying, which avoids the liquid-gas phase change and the associated capillary tension that can collapse weakened wood cells [9]. While adverse structural changes in WAW are predominantly attributed to drying forces, in theory, they can also occur due to other factors occurring during the wood's initial "life" and use or due to osmotic pressure during the impregnation process [6-7]. However, the exact causes can be difficult to determine if the internal structure of wood material is only evaluated after conservation.

Traditionally, treatment success has been evaluated by comparison of the volume of an object pre- and post-treatment [10]. However, recent work performed by the CuTAWAY project used micro-CT to monitor the internal condition of treated WAW samples and evaluate the success of various conservation methods based on the extent of collapse, cracking and shrinkage present [11]. This project revealed that internal damage was present in samples from all treatment methods to varying extents. Even some samples with low to no volume change, previously considered examples of highly successful treatments, had adverse internal structural changes. This highlights the need for additional methods to evaluate the treatment of WAW, particularly regarding monitoring the internal condition.

While micro-CT offers state-of-the-art, unparalleled, high-resolution 3D scans of WAW's internal and external conditions, it is an instrument few conservation labs can access, and even fewer have the funds to operate consistently. The acquisition and subsequent computer generation of these 3D models require specialist skills and equipment and are time-intensive processes.

Alternatively, conservation labs widely use X-rays to create fast 2D representations of the 3D internal structure of heritage objects [12]. X-ray images may, therefore, offer a more commonly available, lower-resolution, low-cost screening alternative to micro-CT scanning of WAW. This paper aims to investigate the applicability of X-rays to monitor the internal condition of WAW before, during and after conservation treatment. This research employs two different methodologies: (1) wet, WAW samples with artificially induced internal damage will

be characterised and X-ray imaged, both before and after impregnation with 40 % PEG 2000; (2) X-ray images of dry, conserved samples will be compared with micro-CT scans of the same samples.

Drying defects in wood

There are numerous types of drying defects with multiple, often overlapping, labels assigned to them [13]. This paper will group the internal drying defects into the following general categories for ease of interpretation (Figure 1):

- Checking – Separation of the wood cell walls, primarily oriented in the radial direction [14-15]. The length and extent of associated delamination vary;
- Ring-shake – Separation of the wood cell walls that run parallel to a tree ring [16]. Like checking, the length and extent of associated delamination vary;
- Intra-ring checking – Small, ellipse-shaped internal cavities that develop within a single growth ring and do not extend significantly beyond [17];
- Macroscopic collapse – Large internal cavities not restricted to a single growth ring. While generally elliptical, the shape tends to be more irregular than intra-ring checking. The area around the edges of the cavities is heavily composed of high-density collapsed cells [18].

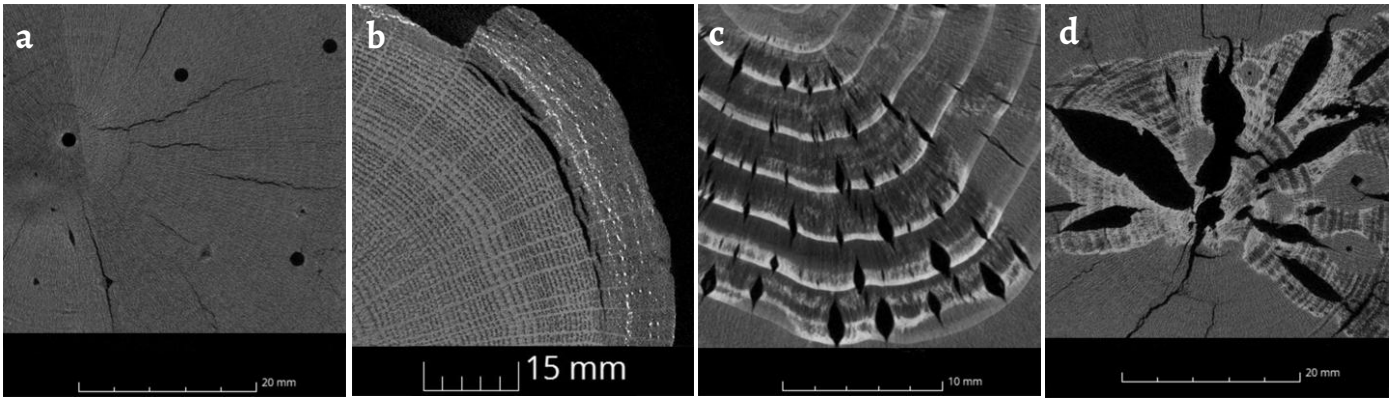

Figure 1. Micro-CT images showing the types of internal damage common in treated waterlogged archaeological wood: *a)* radial checking; *b)* ring-shakes; *c)* intra-ring checking; *d)* macroscopic collapse (photos: D. Gwerder – Lucerne University of Applied Scienced and Arts - HSLU, J. Stelzner and J. Harvie)

Material

Two wet, untreated WAW samples were used to investigate the applicability of X-rays to monitor the internal condition of waterlogged archaeological wood before and during treatment. These samples (UNT1 and PEG1) are deaccessioned wood stem sections obtained from Danish excavations and provided to the Royal Danish Academy for research.

The dry, treated WAW samples used for analysis were selected from the KUR project reference collection at Leibniz-Zentrum für Archäologie (LEIZA). The associated database is available in open access [19]. The database provides the most comprehensive and well-documented collection of conserved WAW, consisting of 21 sample series with over 700 wood samples.

The CuTAWAY project used a sub-selection of this reference collection to evaluate the conserved wood samples using, for example, structured light 3D scans and micro-CT. For this evaluation, where possible, the ten largest samples from each of the eight treatment methods and the untreated control group were selected. A total of 83 samples of the KUR project's databank were analysed by the CuTAWAY project [11].

Table 1. Wood material characteristics of the chosen samples from the KUR Online Databank.

Sample ID	Genus	Size - radial × tangential × longitudinal (mm) measured by callipers	Basic density (g/cm³)	Maximum moisture content (%)	Conservation agent	Anti-shrink efficiency (%) measured by 3D scans
V03-28	Pine (*Pinus* sp.)	58.0 × 39.2 × 74.3	n/a	n/a	Lactitol/Trehalose	87.2
V03-35	Pine (*Pinus* sp.)	47.4 × 52.9 × 74.7	n/a	n/a	PEG 2000	90.1
V07-Exp.3	Beech (*Fagus* sp.)	56.3 × 43.2 ×72.2	0.16	566	Lactitol/Trehalose	92.3
V10-06	Oak (*Quercus* sp.)	53.3 × 51.8 × 86.1	0.38	198	Melamine formaldehyde	78.5
V10-29	Oak (*Quercus* sp.)	50.5 × 53.7 × 91.7	0.41	179	PEG 2000	81.9
V10-39	Oak (*Quercus* sp.)	44.5 × 46.8 × 93.8	0.4	181	PEG 400, PEG1500 & PEG 4000	79.2
V24-56	Alder (*Alnus* sp.)	17.3 × 20.9 × 90.2	0.11	807	Silicone Oil	89.1
V27-07	Oak (*Quercus* sp.)	18.7 × 23.7 × 66.6	0.14	646	Melamine formaldehyde	99.2
V28-10	Ash (*Fraxinus* sp.)	32.0 × 27.5 × 79.4	0.08	1195	PEG 400 & PEG 3350	101.6
V28-24	Ash (*Fraxinus* sp.)	46.0 × 49.5 × 76.7	0.1	983	Silicone Oil	88
V28-36	Ash (*Fraxinus* sp.)	33.5 × 35.8 × 74.4	0.1	929	PEG 400, PEG1500 & PEG 4000	102.6
V30-15	Fir (*Abies* sp.)	23.0 × 20.2 × 68.0	0.16	554	PEG 400, PEG1500 & PEG 4000	94.6
V30-18	Fir (*Abies* sp)	29.6 × 19.6 × 71.3	0.14	632	PEG 400 & PEG 3350	100.1

From the CuTAWAY project's sub-selection, this study selected 13 samples from the 83 analysed. These samples were selected to represent a range of conservation methods, genera, degrees of degradation, and internal damage types. The selected samples varied in condition, from severe internal collapse and checking to little/no adverse structural changes. The wood material characteristics of the chosen samples were obtained from the KUR Online Databank (Table 1) [19].

Samples preparation

The wet, untreated samples (UNT1 and PEG1) were cut into three sub-samples (A, B, and C) using a cordless reciprocating saw (Makita LXT XPT) and a bandsaw (Metabo BAS 318) (Figure 2). Two even-sized sub-samples (A and B) for X-ray analysis and the remaining sample material (C) for material analysis. The sub-samples A and B measured approximately 80 × 110 × 110 mm (UNT1-A&B) and 90 × 120 × 130 mm (PEG1-A&B).

The PEG1 sub-samples were impregnated with PEG 2000 following the Danish Method [9]. The sub-samples were immersed in a solution of 10 % PEG 2000 (Clariant AG) in tap water, followed by 10 % steps of PEG 2000 concentration, ending with a final impregnation solution of 40 % PEG 2000 in tap water (w/v).

To mimic internal damage within the centre of the wood UNT1-A and PEG1-A were cut in half across the grain, and UNT1-B and PEG1-B were split in half along the direction of the wood fibre (Figure 2). A hand drill with a 5 mm diameter drill bit was then used to drill a 10 mm deep hole into the centre of each sub-sample. One oriented longitudinally (A), and the other radially (B) (Figure 2 – red markings). The sub-samples' sides were then fastened along the cut line, wrapping the sample in painter's tape. This was done to restore the sample's original depth and shape, using low-density painter's tape so as not to influence the X-ray images.

Sub-samples for material analysis were obtained by cutting sectors from the wood cross-sections from sub-sample C and dividing them roughly into two equal parts (c. 10-25 g wet weight), representing the interior and exterior wood material for specific material analysis.

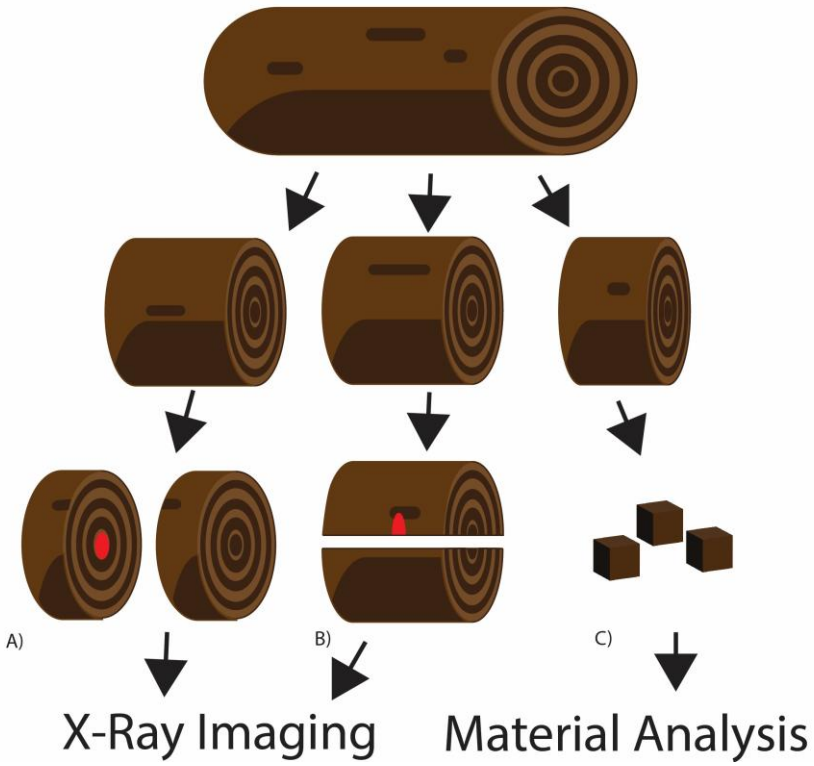

Figure 2. Diagram showing the preparation procedure for samples UNT1 and PEG1. Both samples were cut into three sub-samples (A, B, and C). One sub-sample was cut in half across the grain (A), and the other (B) was split in half along the direction of the wood fibre. Red markings show the approximate placements of drilled holes to mimic internal damage. The third sub-sample (C) was used for wood characterisation analysis.

Methods

Material characterisation of wet samples

Genus identification

To determine the wood genera of UNT1 and PEG1, thin sections (8-15 µm) in transverse, radial and tangential longitudinal directions were taken directly from the wet sample using a razor blade and a microtome (Reichert, model number 361 790). The thin sections were stained with 0.1 % (w/w) Safranin O in water to enhance wood structural features [20], embedded in water, and viewed under a Leica DM750P light microscope with a magnification of ×400. Key anatomical features were used to identify wood genera [21-22].

Basic density and maximum moisture content

The basic density and maximum moisture content were determined for a sub-sample of the interior and exterior wood material of both samples UNT1 and PEG1, as described by Jensen and Gregory [23].

The wet samples' mass (m_{wet}) and volume (V) were measured after the samples were submerged in water in a glass beaker and subjected to a vacuum to ensure complete waterlogging. The volume of the irregularly shaped samples was obtained by measuring the buoyancy force using Archimedes' principle.

$$V = \frac{M_{up}}{\rho_{lfree}}$$

M_{up} = mass of displaced volume of waterlogged sample (g)
P_{lfree} = mass of water per volume of free water (g/cm³)

The samples were then dried in an oven (WTC binder FED) at 105 °C until a stable mass (m_{dry}) was reached (Mettler Toledo ML204 Scale), removing all the free and bound water from the wood structure and obtaining the mass of the remaining wood substance (m_{dry}).

Basic density and maximum moisture content values were then found using the following formulae:

Basic density:

$$\rho_b = \frac{m_{dry}}{v}$$

Maximum moisture content:

$$U_{max} = \frac{m_{wet} - m_{dry}}{m_{dry}} \times 100$$

Ash content

The ash content of the sub-samples was determined using the laboratory analytical procedure established by the National Renewable Energy Laboratory [24]. The samples were held in lidded porcelain crucibles and placed in a muffle furnace (Nabertherm GmbH B410), in which they were subjected to temperatures up to 575 °C and subsequently cooled in a desiccation chamber before the mass was determined (Mettler Toledo ML204 Scale). Heating at 575 °C lasted until a stable mass was obtained for all samples.

The following formula was used to obtain the percentage ash content of the samples:

$$\%\ \text{Ash} = \frac{Weight_{\ crucible\ plus\ ash} - Weight_{crucible}}{m_{dry}} \times 100$$

Imaging of internal structure

X-ray imaging

X-ray images were taken to analyse the wet, untreated WAW samples using a combined analogue/digital solution: computed radiography (CR) and CR scanning (accessible at Royal Danish Academy). The X-ray tube (Andrez Radiation Products AS, Model LSG274) was approximately 45 cm from the phosphorus plate (Blue IP—25 × 40 cm). The optimal operational settings varied with the dimensions of the samples, though the standard operating settings were a voltage of 20-40 kV and a tube current of 2-3 mA at 1 minute radiation time. The imaging plates were scanned using a CR scanner (HD-CR 35 NDT) and the software D-Tect X (Dürr NDT) in the scan mode 25 µm Blue IP / High Res White IP. Subsequent image manipulations could be performed by adjusting the light/contrast/gamma values. However, for the most part, the preinstalled enhancement method "C" was used, increasing contrast for fine structures. X-ray images were taken of each sample in both the radial and longitudinal orientations. Samples PEG1-A and PEG1-B had X-ray images taken before and after impregnation.

X-ray images of the conserved and dried wood samples were obtained with the CT system Phoenix V|tome|x L (Baker Hughes) in 2D mode (accessible at IMPALA, Imaging Platform at LEIZA). A 300 kV microfocus X-ray tube was used, choosing an operation voltage of 120 kV and a tube current of 800 µA with a 0.1 mm copper pre-filter. The radiographical projections were recorded with a dynamic 41|100 detector (410 × 410 mm² detection area and 100 µm pixel size). The distance between the X-ray source and the sample was 168 mm, and between the X-ray source and the detector was 190 mm, giving a magnification of 2.3 and a nominal pixel size of 87 µm. The images were subsequently manipulated in Photoshop 25.3.1 8 (Adobe), adjusting the brightness and contrast to investigate the internal condition of the wood samples more effectively.

Micro-CT scanning

The CT measurements used for this study were performed in the CuTAWAY project on a X-ray µCT system (Diondo d2, Germany) (accessible at Lucerne University of Applied Sciences and

Arts, HSLU). The X-ray source (XWT-225 TCHE+ from X-ray works, Garbsen, Germany) was set in high-power mode, and an operation voltage of 120 kV and a tube current of 167 µA with a 1 mm aluminium pre-filter was set. The wood samples were placed in the sample chamber mounted in a sample holder, which allowed them to rotate 360 ° in continuous mode during the acquisition. A 4343 DX-I X-ray detector (Varex, Salt Lake City, USA) was used to record the radiographical projections, with a pixel size of 139 µm. The distance between the X-ray source and the sample was 160-250 mm, and between the X-ray source and the detector was 860 mm. This gave a magnification between 3.4 and 5.4 and a nominal voxel size between 27 and 44 µm. 3000 projection images were acquired during the sample rotation of 360 °.

For the image reconstruction, the projections were combined to establish the distribution of the attenuation in the investigated material and a three-dimensional matrix of the attenuation coefficients was calculated using a reconstruction algorithm [25].

Results

Wet WAW material characteristics

Table 2 shows the results of the performed wood material characteristics and genus identification for samples UNT1 and PEG1.

Table 2. Overview of determined wood characteristics of the wet WAW sample material UNT1 and PEG1.

Sample	Genus	Sample location	Basic density (g/cm³)	Maximum moisture content (%)	Ash content (%)
UNT1	Oak (*Quercus* sp.)	Outer wood	0.09	1074.8	3.9
		Inner wood	0.19	462.4	5.4
		Combined values	0.13	683.5	4.8
PEG1	Spruce (*Picea* sp.)	Outer wood	0.15	588.1	7.7
		Inner wood	0.24	321.8	1.3
		Combined values	0.19	433.0	3.1

The basic densities of both samples are below those of their green wood counterparts, as mean basic density values for green oak (*Quercus* sp.) and spruce (*Picea* sp.) are 0.56 g/cm³ and 0.38 g/cm³, respectively. This suggests moderate to high levels of degradation [26]. Particularly in the surface areas of the samples, which have the most significant levels of degradation present, though the inner cores are degraded too. This is a common occurrence in waterlogged archaeological wood, where the highest levels of degradation, as measured by basic density and maximum moisture content, are found in the outer areas of wood. Based on De Jongs' criteria for categorising the degradation of WAW material by maximum moisture content, both samples are class III (400 %+) or “heavily degraded” [27].

In line with previous studies, the ash content of the waterlogged archaeological wood was also noticeably higher than that of green wood, which has been reported to be around 0.35 % and 0.65 % for spruce (*Picea* sp.) and oak (*Quercus* sp.), respectively [28-29].

However, it should be noted that as both the degradation of WAW and diffusion of inorganic material within the wood structure are not uniform processes, the characterisation of sub-samples can only indicate the general characteristics of an entire sample [30].

X-ray imaging of untreated wet samples

The 5 mm diameter, 10 mm deep holes drilled into samples UNT1-A and UNT1-B to mimic internal damage were visible in the X-ray images as small circular shadows (Figure 3).

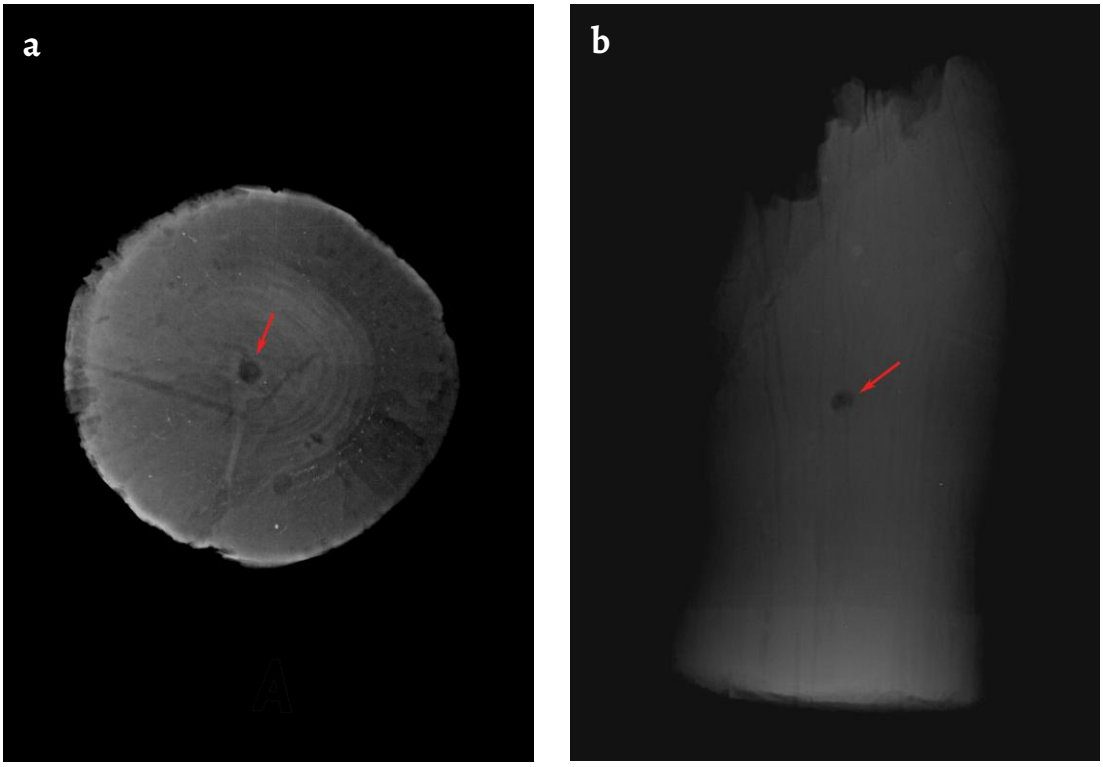

Figure 3. X-ray images of samples: *a)* UNT1-A; *b)* UNT1-B. Induced internal damage is visible as the circular shadow in the centre of both samples (photos: J. Harvie and J. Aagaard).

X-ray imaging of the untreated samples also revealed information about the structure of the wood material itself, visualising existing checks in the wood structure and a layer of material around the surface with higher levels of degradation. These checks likely occurred during the object's initial "life" due to changes in the wood moisture content and associated anisotropic shrinkage or due to mechanical forces exerted on the wood [6]. The X-ray image also appeared to differentiate between the sample's heartwood and sapwood. Heartwood, in some genera, is a denser material due to the accumulation of extractives [26].

X-ray imaging of PEG impregnated wet samples

X-ray images of the PEG1 subsamples, pre- and post-impregnation with 40 % PEG 2000 in water, proved harder to interpret due to the heterogeneous density levels within the wood's internal structure. Unlike the UNT1 subsamples, which had clear areas of low relative density in the external areas of the wood samples due to degradation, the X-ray images of the PEG1 subsamples showed low-density material primarily in the internal structure of the wood. The relatively low density of the internal wood of the PEG1 sub-samples is believed to be due to the increased levels of higher-density minerals present in the outer wood, as identified using the ash content, and the naturally lower density of both juvenile wood in genera such as spruce in comparison to the mature wood material, and earlywood in comparison to high-density latewood [26, 31].

The 5 mm diameter, 10 mm deep holes drilled into samples PEG1-A and PEG1-B to mimic internal damage were visible in the X-ray images as small circular shadows (Figure 4). However, identifying this internal damage was challenging with the current X-ray setup due to the low contrast between the internal damage and the adjacent low-density intact wood material.

The presence of PEG within the wood structure did not significantly affect the ability of X-ray imaging to assess the internal structure of the wood samples.

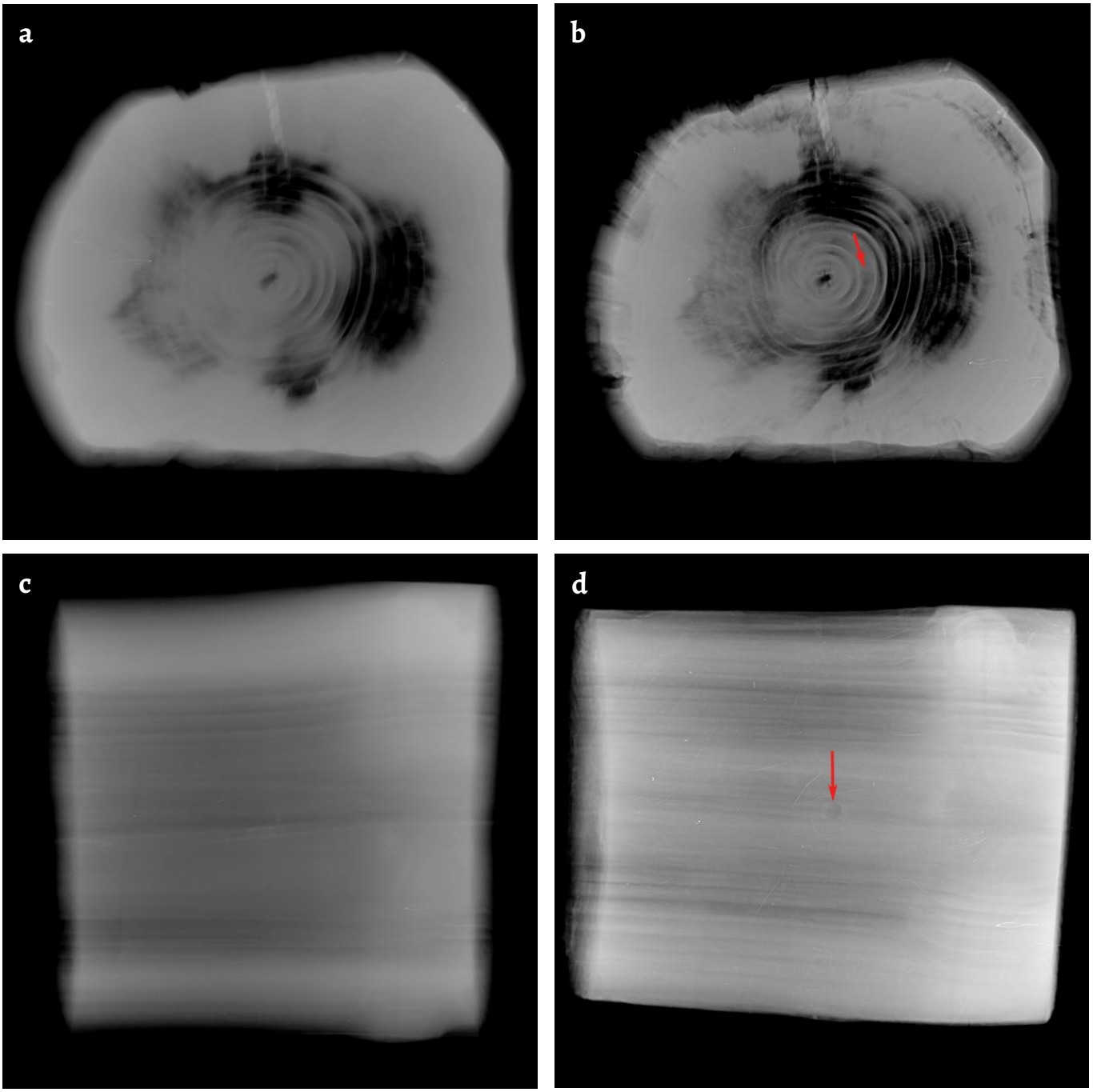

Figure 4. X-ray images of wet PEG-impregnated samples: *a)* PEG1-A pre-impregnation; *b)* PEG1-A post-impregnation; *c)* PEG1-B pre-impregnation; *d)* PEG1-B post-impregnation with artificial damage visible in the wood centre as grey shadow (photo: J. Harvie and J. Aagaard).

X-ray imaging of dry and treated WAW samples

Using the high-resolution micro-CT scans of the treated samples as a reference, the degree to which the X-ray images could assess the internal condition of the treated WAW was identified by describing the qualitative differences between the internal damages visible in the X-ray images and the micro-CT scans (Table 3). While micro-CT 3D scans allow for quantitative analysis of the internal damage present within treated waterlogged archaeological wood, see Stelzner et al. 2023 [11], as X-ray images create a compressed 2D representation of 3D information, only qualitative analysis is possible.

Table 3. Qualitative comparisons of the internal damage in dry, treated archaeological wood samples visible in X-ray images compared to micro-CT scans. Representative images are found in Figure 5 and Figure 6.

Similar		
Samples	**Internal damage visualised by micro-CT scanning and X-Ray imaging**	
V03-35	Long internal radial checks with low levels of associated delamination.	
V28-10 (Figure 6a-d)	Large amounts of macroscopic collapse confined to the centre of the sample structure, with associated denser surrounding material. Small radial checks with limited levels of delamination.	
V28-24	Numerous areas of large macroscopic collapse and associated surrounding high-density material. The collapse extends in areas from the centre to the surface of the sample. Intra-ring checking is also present throughout the sample.	
V28-36 (Figure 5a-b)	Minor and major, primarily radially orientated, checks. Some run from pith to edge, resulting in a void.	
V30-15	Minor radial checks, with 1-2 major checks extending to the surface.	
Minor-moderate variations		
Samples	**Micro-CT**	**X-Ray**
V07-Exp.3	Large and minor radially orientated checks, some with large levels of associated delamination. Minor internal checking/collapse located primarily around the edges of the sample and in the heartwood structure.	The large internal cracks are visible (they may appear to occupy a larger area of the wood structure, though this is likely due to the distortion of the X-ray image). Most of the internal checks/voids are visible.
V10-06	Extremely large ring shake with extreme levels of delamination. Checking in the degraded outer wood.	The delamination associated with the check loses clarity in the exterior areas of high degradation. The fill material used to stabilise the sample post-CT scan is also clearly visible.
V24-56	Radial checks and collapse in the outer wood of the sample. One large check running from edge to pith.	The same internal damage is visible, but the image is far less clear and interpretation more difficult, likely due to the irregular shape of the sample and its orientation during X-ray scanning.
V27-07	Sporadic intra-ring checking, primarily between the outer and inner growth rings. One area of macroscopic collapse. Large radial check has ruptured the wood material from the surface to centre.	Internal checking and the large radial check with associated rupture are clearly visible. However, the macroscopic collapse is difficult to make out due to the busy nature of the X-ray image caused by overlapping areas of internal damage.
V30-18 (Figure 5c-d)	Large amount of internal checking, particularly prominent in one area of the wood structure. Radial checking is present, with limited associated delamination. The largest of which extends from pith to wood surface.	The present internal damages are similarly visible in both the X-ray and micro-CT. However, the irregular shape of the sample makes interpretation more challenging.
Major variations		
Samples	**Micro-CT**	**X-Ray**
V03-28 (Figure 5e-f)	Minor radial checking with extremely low associated delamination, primarily found in the heartwood of the sample.	There is no clear evidence of adverse internal damage.
V10-29 (Figure 6e-h)	Minor, thin, radial checks and ring-shakes, running along the growth rings with minor delamination.	Unable to make out any of the internal checks or shakes. It is particularly difficult to see internal changes in low-density areas as the contrast is so low.
V10-39	Large and minor ring shakes with a great deal of delamination are associated with some. Minor radial checks and small radially orientated voids primarily focused around the heartwood.	Shakes, checks, and internal voids in the less-degraded areas are visible, though to a lesser extent than in the micro-CT. Only the large shakes with associated delamination are visible in the degraded wood on the x-ray.

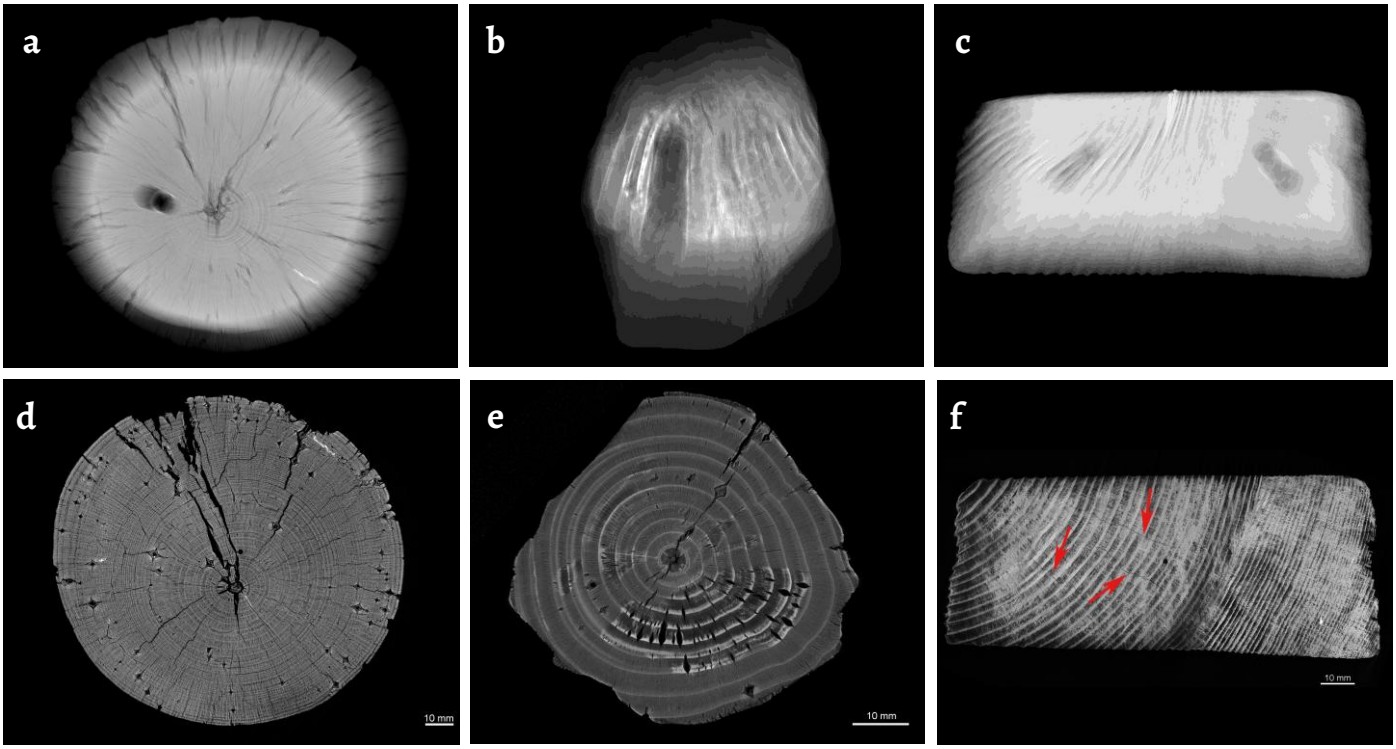

Figure 5. X-ray images of samples: *a)* V28-36; *b)* V30-18; *c)* V03-28 and micro-CT scan samples: *d)* V28-36; *e)* V30-18, and *f)* V03-28; showing the varying ability of X-ray imaging to identify the internal damage visible in micro-CT scans as mentioned in Table 3. The red arrows in Figure 5f highlight the small radial checks visible in the micro-CT scans but not in the X-ray image. Note that the large circular columns in the X-ray images are from the removal of a core sample taken after the micro-CT scan (photo: D. Gwerder, J. Stelzner and J. Harvie)

X-ray images of the treated samples clearly revealed internal damages present in the internal structure of the samples. Particularly prominent in the X-ray images were areas of damage associated with an absence of wood cell wall material, such as intra-ring checking, collapse, and shakes or checks with delamination. This high level of contrast was due to the high difference in density between these voids and the surrounding wood/conservation agent material. In sample V28-10, it was even possible to identify a high-density region surrounding the large areas of collapse, which was likely composed of collapsed cell material (Figure 6a-d). However, X-rays struggled to resolve the difference between areas of internal damage with little related material voids, such as minor checking or shakes, especially those present in the degraded regions of the samples where the material was low density due to degradation (Figure 6e-h). This was partly due to the lower resolution of this method compared to micro-CT and the low levels of difference in density between the area of damage and the sound wood.

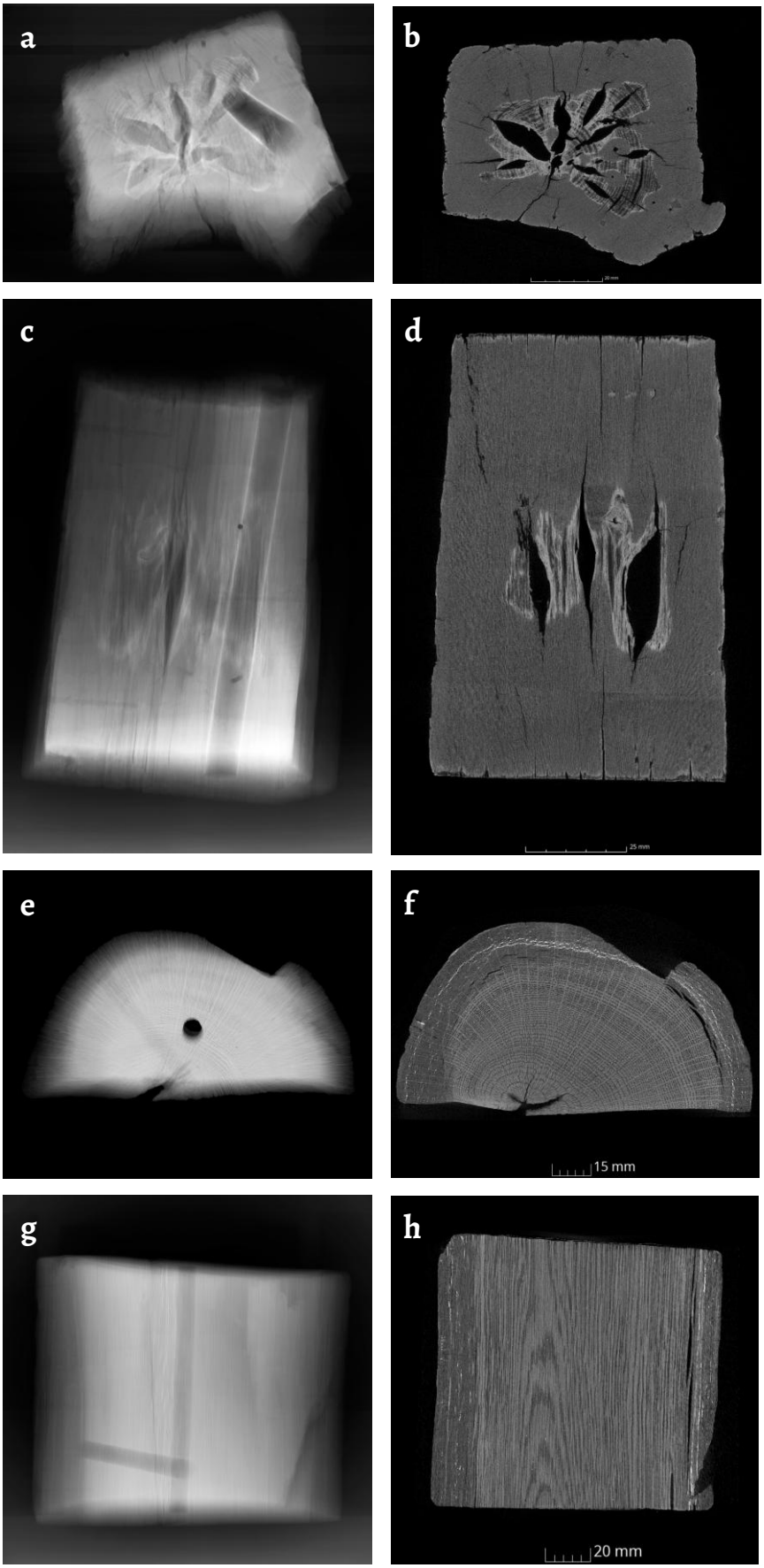

Figure 6. X-ray images (left) and micro-CT scan (right) of sample V28-10: *a-b*) transversal and *c-d*) longitudinal directions; and sample V10-29: *e-f*) transversal and *g-h*) longitudinal directions. Sample V28-10 shows high levels of collapse and radial checks in both the X-ray and Micro-CT images (Figure 6a-d). Whereas Figure 6e-h of sample V10-29 show that the moderate ring shakes in the micro-CT are not clearly visible in the X-ray. Note that the large circular columns in the X-ray images are from the removal of a core sample taken after the micro-CT scan (photo: D. Gwerder, J. Stelzner and J. Harvie).

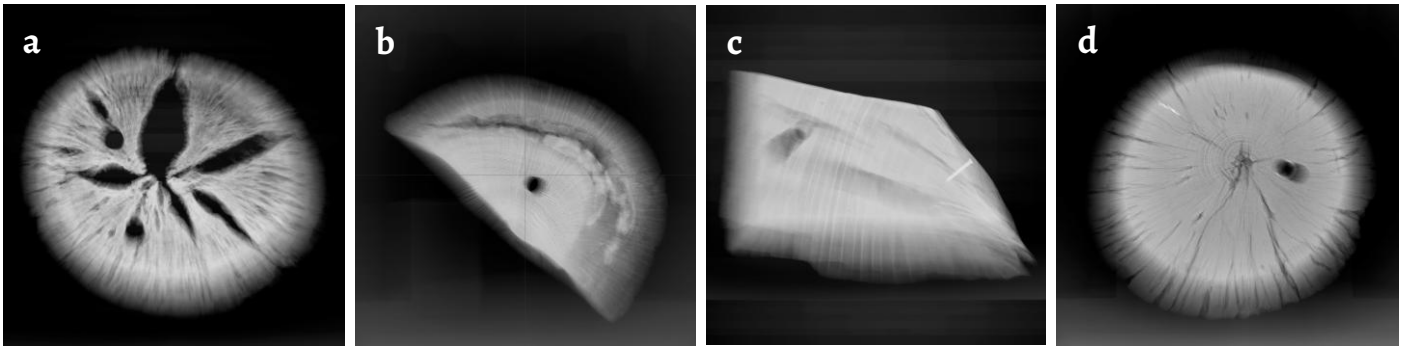

Figure 7. X-Ray images of waterlogged archaeological wood samples treated with various conservation agents: *a)* silicone oil; *b)* melamine formaldehyde (Kauramin 800); *c)* lactitol – trehalose; *d)* PEG. Further information on sample treatments is available [19] (photo: J. Stelzner and J. Harvie (RDA).

The ability of the X-ray to assess the internal condition of the wood samples was not limited by the conservation agent used, though methodology adjustments were required depending on the sample; for example, those treated with higher-density silicon oil required a higher kV to penetrate the conservation agent (Figure 7).

Discussion

X-ray imaging proved reliable in identifying the majority of internal damages present in the WAW samples at all stages of conservation. Particularly the larger damages that may impact WAW objects' subsequent stability and analysis. This method was also significantly faster than micro-CT scanning. Each image took between 15 and 25 minutes, including subsequent editing for image optimisation.

However, X-ray images present a 2D representation of a 3D sample, showing the accumulated expression of its total density. This can lead to misinterpretations, as areas of high internal damage that dominate the X-ray image may be localised rather than widespread throughout the wood. Layers of multiple internal damages may also be difficult to individually identify and differentiate between. Multiple-angle X-ray imaging can partially negate this, but even this method cannot match the clarity and resolution of 3D micro-CT scans, which allows the entire sample volume to be examined at various spatial resolutions [32].

The results of this research highlighted that challenges to interpreting X-ray images of WAW can also arise due to the heterogeneous nature of the material's density. The density of individual waterlogged archaeological wood samples varies between genera, levels of degradation, and conservation treatment type, which can be accounted for by changing the operational settings of the X-ray as necessary. However, variations in internal density within the same sample are not only attributable to internal damage. Numerous factors result in large variations in density, including growth variations and genus-specific internal variability, which are well documented in green wood [26]. For example, the juvenile wood of some genera can have a significantly lower density than the mature wood – 391 kg/m^3 to 552 kg/m^3 in pine wood [31]. Other factors contributing to high variations in the density of WAW material occur during deposition. The primary degraders of WAW attack the wood structure from the surface inwards, using rays and piths as transport pathways, degrading the wood material in a non-uniform manner [4]. The diffusion of high-density, inorganic minerals into the wood material structure during deposition also occurs unevenly [33].

These factors could result in the presence of darker (low relative density) patches in X-ray images that can obscure instances of internal damage or be incorrectly attributed as such themselves. Therefore, conservators must be aware of these variations to correctly use X-ray imaging to assess the internal condition of waterlogged wood at any stage of conservation treatment.

Conclusion

X-ray images proved to be an appropriate method to assess the internal condition of waterlogged archaeological wood pre-, intra-, and post-conservation. Areas of low, moderate, and high internal damage were visible as areas of low-density dark spots, particularly prominent when associated with voids in the material. The visibility of the characteristic features of internal damage in wood due to drying, such as the delamination of wood material orientated along the growth rings and the high-density cell material associated with macroscopic collapse, allowed for specific macroscopic internal damages to be identified and characterised. Highlighting X-ray as a low-resolution, fast alternative to micro-CT. Though micro-CT remains the state-of-the-art method for assessing the internal condition of WAW.

However, the interpretation of X-ray images to assess the internal condition of WAW can pose challenges. These challenges can generally be divided into those caused by the limitations of the technique and those resulting from the numerous potential causes for internal density variation, aside from internal damage due to the heterogeneity of the material. In order to overcome these challenges, an underlying understanding of the nature of the material is required.

Acknowledgements
I want to thank all those involved with the KUR and CuTAWAY projects [11, 19] for their work, which made this research possible. Finally, I thank the Kalmerfonden Scholarship for funding my research trip to LEIZA, Mainz, Germany.

Data availability statement
Further information on the wood samples is available online at https://www1.rgzm.de/kur/ . Cross-sectional images from x-ray computed tomography (XCT) of conserved samples are available on the Zenodo repository, doi: 10.5281/zenodo.12690015.

REFERENCES

1. Kaye, B., 'Conservation of waterlogged archaeological wood', *Chemical Society Reviews* **24**(1) (1995) 35-43, https://doi.org/10.1039/CS9952400035.
2. Historic England, *Waterlogged wood: guidelines on the recording, sampling, conservation and curation of waterlogged wood*, Historic England Publications, Swindon (2010), https://historicengland.org.uk/images-books/publications/waterlogged-wood/ (accessed 2024-10-30).
3. Pedersen, N. B., *Microscopic and spectroscopic characterisation of waterlogged archaeological softwood from anoxic environments*, University of Copenhagen, Frederiksberg (2015).
4. Singh, A, P., 'A review of microbial decay types found in wooden objects of cultural heritage recovered from buried and waterlogged environments', *Journal of Cultural Heritage* **13**(3) (2012) 16-20, https://doi.org/10.1016/j.culher.2012.04.002.
5. Haque, N., 'Delamination in timber induced by drying', in *Delamination in Wood, wood products and wood-based composites*, ed. V. Bucur, Springer Netherlands, Dordrecht (2011) 197-212, https://doi.org/10.1007/978-90-481-9550-3_10.
6. Fu, Z.; Jiaxing, C.; Yongyue, Z.; Feifan, X.; Yun, L. 'Review on wood deformation and cracking during moisture loss', *Polymers* **15**(15) (2023) 3295, https://doi.org/10.3390/polym15153295.
7. Grattan, D. W.; Clarke, R. W., 'Conservation of waterlogged wood', in *Conservation of marine archaeological objects*, ed. C. Pearson, Butterworths, London (1987) 164-206, https://doi.org/10.1016/B978-0-408-10668-9.50015-0.
8. Jensen, P., 'Sorption of water and water soluble agents in the waterlogged wooden cell wall', in *Proceedings of the 6th ICOM Group on wet organic archaeological materials conference*, eds. P. Hoffmann, T. Daly, T. Grant & J. Spriggs, Druckerei Ditzen GmbH und Co., Bremerhaven (1997) 399-434.
9. Strætkvern, S., 'Vacuum freeze-drying of waterlogged archaeological wood and selecting the impregnation agent prior to drying', in *Proceedings of the international experts' meeting on the extraction and conservation of the Wreck Mazarrón 2*, eds. M. A. Garcia, R. C. Belinchon & C. C. Escribano, Ministerio de Cultura, Madrid (2023) 303-314.
10. Johns, D. A., 'Post-excavation treatment methods for waterlogged organic archaeological materials: the last twenty years', in *The Oxford handbook of wetland archaeology*, eds. F. Menotti & A. O'Sullivan, Oxford Academic, Oxford (2012) 664-684, https://doi.org/10.1093/oxfordhb/9780199573493.013.0040.
11. Stelzner, I.; Stelzner, J.; Martinez-Garcia, J.; Gwerder, D.; Wittköpper, M.; Muskalla, W.; Cramer, A.; Heinz, G.; Egg, M.; Schuetz, P., 'Evaluation of conservation methods for archaeological wet wood with structured light 3D scanning and μ-CT', in *Proceedings of the 15th ICOM-CC Group on wet organic archaeological materials conference*, eds. I. Hovmand, M. Felter & I. Stelzner, ICOM-CC, Mainz (2023) 96-105.
12. Mardikian, P.; Chemello, C., 'Conservation laboratory design', in *Encyclopedia of global archaeology*, ed. C. Smith, Springer, Cham (2018) 1-7, https://doi.org/10.1007/978-3-319-51726-1_433-2.

13. Evans, P. D., 'The effects of incising on the checking of wood: a review', *International Wood Products Journal* **7**(1) (2016) 12-25, https://doi.org/10.1080/20426445.2015.1112936.
14. Yang, D-Q.; Normand, D., *Best practices to avoid hardwood checking Part I. Hardwood checking – the causes and prevention*, FPInnovations - Transorfmative Technologies Program, Quebec (2012).
15. Pearson, H.; Donaldson, L.; Kimberley, M.; Davy, B., 'Supercritical CO_2 drying of New Zealand Red Beech to below the fibre saturation point reduces collapse distortion', *Wood Science and Technology* **58**(2) (2024) 459-483, https://doi.org/10.1007/s00226-023-01509-y.
16. Richter, C., 'Overview of cracks/shake forms and causes', in *Wood characteristics: description, causes, prevention, impact on use and technological adaptation*, ed. C. Richter, Springer International Publishing, Cham (2015) 199-208, https://doi.org/10.1007/978-3-319-07422-1_8.
17. Putoczki, T. L.; Nair, H.; Butterfield, B.; Jackson, S. L., 'Intra-ring checking in Pinus Radiata D. Don: the occurrence of cell wall fracture, cell collapse, and lignin distribution', *Trees* **21**(2) (2007) 221-229, https://doi.org/10.1007/s00468-006-0114-y.
18. Grattan, D. W., 'Waterlogged wood', in *Conservation of marine archaeological objects*, ed. C. Pearson, Butterworths, London (1987) 55-67, https://doi.org/10.1016/B978-0-408-10668-9.50009-5.
19. 'Mass Finds in Archaeological Collections', in *RGZM*, https://www1.rgzm.de/kur/ (accessed 2024-03-13).
20. Bond, J.; Donaldson, L.; Hill, S.; Hitchcock, K., 'Safranine fluorescent staining of wood cell walls', *Biotechnic & Histochemistry* **83**(3-4) (2008) 161-171, https://doi.org/10.1080/10520290802373354.
21. Wheeler, E.; Baas, P.; Gasson, P., 'IAWA list of microscopic features for hardwood identification', *IAWA Bulletin* **10**(3) (1989) 219-332.
22. Richter, H. G.; Grosser, D.; Heinz, I.; Peter, E., 'IAWA list of microscopic features for softwood identification', *IAWA journal* **25**(1) (2004) 1-70.
23. Jensen, P.; Gregory, D. J., 'Selected physical parameters to characterize the state of preservation of waterlogged archaeological wood: a practical guide for their determination', *Journal of Archaeological Science* **33**(4) (2006) 551-559, https://doi.org/10.1016/j.jas.2005.09.007.
24. Sluiter, A.; Hames, B.; Ruiz, R.; Scarlata, C.; Sluiter, J.; Templeton, D., 'Determination of ash in biomass (NREL/TP-510-42622)', in *National Renewable Energy Laboratory Technical Report 19*, National Renewable Energy Laboratory, Golden Colorado (2005).
25. Feldkamp, L. A.; Davis, L. C.; Kress, J. W., 'Practical cone-beam algorithm', *Journal of the Optical Society of America* **A1** (1984) 612-619.
26. Niemz, P.; Sonderegger, W.; Keplinger, T.; Jiang, J.; Lu, J., 'Physical properties of wood and wood-based materials', in *Springer handbook of wood science and technology*, eds. P. Niemz, A. Teischinger & D. Sanberg, Springer International Publishing, Cham (2023) 281-353.
27. de Jong, J., 'Conservation techniques for old archaeological wood from shipwrecks found in the Netherlands', in *Biodeterioration investigation techniques*, ed. A. H. Walters, Applied Science, London (1977) 295-338.
28. Hedges, J. I., 'The chemistry of archaeological wood', in *Archaeological wood. properties, chemistry and preservation*, eds. R. M. Rowell & R. J. Barbour, American Chemical Society, Washington D. C. (1990) 111-139.
29. Passialis, C. N., 'Physico-chemical characteristics of waterlogged archaeological wood', *Wood Research and Technology* **51**(2) (1997) 111-113, https://doi.org/10.1515/hfsg.1997.51.2.111.
30. McConnachie, G.; Eaton, R.; Jones, M., 'A re-evaluation of the use of maximum moisture content data for assessing the condition of waterlogged archaeological wood', *E-preservation Science* **5** (2008) 29-35.
31. Gryc, V.; Vavrčík, H.; Horn, K., 'Density of juvenile and mature wood of selected coniferous species', *Journal of Forest Science* **57**(3) (2011) 123-130, https://doi.org/10.17221/18/2010-JFS.
32. Withers, P. J.; Bouman, C.; Carmignato, S.; Cnudde, V.; Grimaldi, D.; Hagen, C. K.; Maire, E.; Manley, M.; Du Plessis, A.; Stock, S.R., 'X-ray computed tomography', *Nature Reviews Methods Primers* **1** (2021) 18, https://doi.org/10.1038/s43586-021-00015-4.
33. Almkvist, G.; Persson, I.,'Extraction of iron compounds from wood from the Vasa', *Holzforschung* **60**(6) (2006) 678-684, https://doi.org/10.1515/HF.2006.114.

RECEIVED: 2024.12.1
REVISED: 2025.3.7
ACCEPTED: 2025.6.1
ONLINE: 2026.3.8